Polymer 51 (2010) 2668–2675

Contents lists available at ScienceDirect

Polymer

journal homepage: www.elsevier.com/locate/polymer

Drug release kinetics from monolayer films of glucose-sensitive microgel

Pengxiao Liu, Qiaofang Luo, Ying Guan, Yongjun Zhang*

Key Laboratory of Functional Polymer Materials, Institute of Polymer Chemistry, College of Chemistry, Nankai University, Tianjin 300071, China

ARTICLE INFO

Article history:
Received 14 October 2009
Received in revised form
2 April 2010
Accepted 8 April 2010
Available online 1 May 2010

Keywords:
Microgels
Glucose-sensitive
Drug delivery

ABSTRACT

To study the drug release behaviors of glucose-sensitive poly(N-isopropylacrylamide-co-3-acrylamidophenylboronic acid) (P(NIPAM-PBA)) microgels, P(NIPAM-PBA) microgel monolayers were prepared by the modification of poly(N-isopropylacrylamide-co-acrylic acid) microgel monolayers with 3-aminophenylboronic acid under EDC catalysis. Alizarin Red S (ARS) and FITC-labeled insulin (FITC-insulin) were loaded in the monolayers respectively. Their release kinetics under various conditions were measured. For both drugs, at low temperature, the drug release can be described as passive diffusion of the drugs. At temperature higher than the phase transition temperature, however, the drugs are released via a "squeeze-out" mechanism. Glucose-regulated release for both drugs was observed. At all temperatures glucose enhances the release of ARS because it competes with ARS for binding with PBA groups. For FITC-insulin, glucose enhances its release at 4 °C, but retards at 37 °C. These results will guide the design of self-regulated insulin release systems based on P(NIPAM-PBA) microgels.

1. Introduction

Self-regulated insulin release systems, as artificial pancreas, deliver suitable amount of insulin according to the blood glucose level in diabetic patients [1,2]. Therefore these systems may provide better control over blood glucose level and thus reduce the incidence of dangerous complications. Glucose-sensitive hydrogels play a key role in the design of such systems [3,4]. Although the systems based on proteins, such as glucose oxidase and concanavalin A, have the advantage of high selectivity, they also suffer from poor stability, toxicity, and potential antigenicity in vivo [3]. In contrast, totally synthesized hydrogels using phenylboronic acid (PBA) groups as glucose-sensitive moiety are more stable. Self-regulated insulin release has been achieved from these hydrogels [3]. They have further been improved to operate at physiological pH [5,6].

Recently, we and others synthesized PBA-bearing microgels which present glucose-sensitive swelling behaviors [7–9]. Compared with their bulky analogues, due to their reduced size, these microgels may response more quick to changes in blood glucose level. The monodisperse microgel particles have been used as building blocks for the fabrication of polymerized crystalline colloidal array glucose biosensors [10]. Some efforts have also been made to exploit their ability as insulin delivery vehicles [11,12]. In a previous work, we demonstrated that the permeability of the microgels can be tuned by glucose concentration, suggesting these materials have great potential for the application for self-regulated insulin release [13]. To design a self-regulated insulin release system based on these microgels, knowledge about the drug release mechanism is indispensable. Unfortunately we know little about this, while the drug release mechanism of bulky hydrogels has been studied extensively in the literature. Because of their size difference, microgels may present drug release behaviors different from that of bulky gels.

A reason for this situation may be the difficulty to experimentally measure the kinetics of drug loading and release, which is crucial for the understanding of the drug release mechanisms. To study the drug loading and release behavior of colloidal particles, a commonly used method is the so-called "solution-depletion" method, in which the microgel particles are separated by centrifugation and the drug concentration in the supernatant is measured [14,15]. With this time-consuming method, it is hard to trace the quick drug loading and release. Some authors put the colloidal suspension in a dialysis bag and measure the drug concentration outside the bag [16]. However, drug starts to release immediately once it contact the media, therefore, the kinetics results from this method will not be accurate. To circumvent these problems, the colloidal particles can be immobilized on a macroscopic solid base, so their manipulation will be much easier. Quick and accurate measurement of drug loading and release will be possible. Previously single microgel particles were immobilized at the end of a micropipette [17]. This method may only be applicable for particles with a relatively large size (particles with a diameter of 6.5 μm were immobilized and manipulated in Ref [17]). On the other hand, Lyon et al self-assembled microgel particles into

* Corresponding author. Tel.: +86 22 23501657; fax: +86 22 23503510.
E-mail address: yongjunzhang@nankai.edu.cn (Y. Zhang).

0032-3861/$ – see front matter © 2010 Elsevier Ltd. All rights reserved.
doi:10.1016/j.polymer.2010.04.011

multilayer films using the layer-by-layer assembly technique [18,19]. The release of insulin [18] and doxorubicin [19] from these thin films was studied. However, since the microgel particles were complexed with a cationic polyelectrolyte and embedded inside multilayer films, their properties may be altered and very different from those dispersed in solution. To reduce the alteration on the particle properties, here we synthesized microgel monolayers. Compared with the dispersed particles, when immersed in solutions, the environment of the particles is largely remained. Using this method we studied the drug loading and release behavior of P(NIPAM-PBA) microgels. The mechanisms of drug release from the microgel particles were proposed. The results show that the drug release can be regulated by glucose concentration.

2. Experimental section

2.1. Materials and apparatus

N-isopropylacrylamide (NIPAM) was purchased from Acros. 3-Aminophenylboronic acid hemisulfate (APBA), 1-(3-dimethylaminopropyl)-3-ethylcarbodiimide hydrochloride (EDC), N, N′-methylenebisacrylamide (BIS) and polyethyleneimine (PEI) were purchased from Alfa Aesar. 5-Isothiocyanate fluorescein (FITC) and insulin were purchased from Newprobe. Alizarin red S (ARS), acrylic acid (AA) and ammonium persulfate (APS) were purchased from local providers. NIPAM was purified by recrystallization from a hexane/acetone mixture and dried in a vacuum. AA was distilled under reduced pressure. FITC-insulin was prepared from FITC and insulin according to Ref [20]. Other chemicals were of analytical grade and used as received.

The size of the microgel particles was measured by dynamic light scattering with a Brookhaven 90Plus laser particle size analyzer. All the measurements were carried out at a scattering angle of 90°. The sample temperature was controlled with a build-in Peltier temperature controller. SEM images were recorded on a SHIMADZU Superscan SS-550 scanning electron microscope. The samples were sputter coated with PdAu before the imaging. Fourier transform infrared (FTIR) spectra were measured on a Bio-Rad FTS-6000 spectrometer. UV–vis absorption spectra were measured on a TU 1810PC UV–Vis spectrophotometer (Purkinje General, China). Fluorescence spectra were measured on a SHIMADZU RF-5301PC spectrofluorophotometer using an excitation wavelength of 490 nm.

2.2. Synthesis of P(NIPAM-AA) and P(NIPAM-PBA) microgels

Poly(N-isopropylacrylamide-co-acrylic acid) (P(NIPAM-AA)) microgels were prepared by surfactant-free emulsion polymerization, following a procedure described by Pelton and Chibanate [21]. Briefly, 1.400 g of NIPAM, 0.100 g of AA and 0.033 g of BIS were dissolved in 100 mL of water. The reaction mixture was transferred to a three-necked round-bottom flask equipped with a condenser and a nitrogen line. The solution was purged with nitrogen for about 10 min and then heated to 70 °C. After 1h, 5 mL of 0.06 M APS solution was added to initiate the reaction. Within 10 min, the solution turned turbid, indicating the nucleation of particles. The reaction was allowed to proceed for 6 h. The resultant microgels were purified by dialysis (cutoff 8000–15000) against water with at least twice daily water changes for at least 1 week.

Poly(N-isopropylacrylamide-co-3-acrylamidophenylboron-ic acid) P(NIPAM-PBA) microgels were prepared by modifying the P(NIPAM-AA) microgels with APBA [7]. Briefly, 5 mL of purified P(NIPAM-AA) microgels was added to 45 mL of aqueous solution containing 0.233 g of APBA and 0.239 g of EDC at 0 °C. The reaction was allowed to proceed for 4 h. The resultant microgels were dialyzed against water for 2 days.

2.3. Preparation of P(NIPAM-AA) and P(NIPAM-PBA) microgel monolayers

A procedure described by Vincent et al. [22] was followed to prepare the P(NIPAM-AA) microgel monolayers. The monolayers for SEM characterization were fabricated on silicon wafers. Other monolayers were fabricated on quartz slides with a size of 44 mm × 10 mm × 1 mm. Before use, both substrates were cleaned with piranha solution (3:7 v/v H_2O_2–H_2SO_4 mixture) for 2 h (*caution: this solution is extremely corrosive!*), followed by rinsing with deionized (DI) water. The substrates were then modified with PEI by dipping into a 10 wt.% PEI solution for 10 min followed by thorough rinsing with DI water. The P(NIPAM-AA) microgel monolayers were prepared by soaking the PEI-modified substrates in a dispersion containing 1.5 wt.% microgel and 10 mM KCl, which was preheated to 50 °C, for 5 min. After rinsing in water for 15 min, the microgel monolayers were dried in air.

The P(NIPAM-PBA) microgel monolayers were prepared by modifying the P(NIPAM-AA) microgel monolayers with APBA under EDC catalysis. To this end, 0.116 g of APBA and 0.120 g of EDC were dissolved in 60 mL of water and cooled to 0 °C. P(NIPAM-AA) microgel monolayers were immersed in the solution for 4 h. The resultant monolayers were washed with DI water thoroughly and dried.

2.4. Loading and release of ARS

The P(NIPAM-PBA) microgel monolayers were immersed in ARS solutions in phosphate buffer (50 mM, pH 8.5). At proper intervals, the films were taken out, soaked in DI water briefly and dried. The loading amount of ARS was determined by UV–vis spectroscopy. When loaded in 50 mM ARS, from the increase in monolayer weight, the weight percentage of loading was estimated to be ~16%.

To measure the release kinetics of ARS, ARS was first loaded by immersing the microgel monolayers in 10 mM ARS in phosphate buffer (50 mM pH 8.5) at 4 °C for 1 h. They were briefly washed with DI water of the same temperature and then soaked in 15 mL of release media with different composition and temperature. At predetermined intervals the media were sampled. The concentration of ARS was measured by UV–vis spectroscopy. The samples were returned after measurement to keep a constant volume of release media. Temperature of the release media was controlled with a refrigerated circulator.

2.5. Loading and release of FITC-insulin

FITC-insulin was loaded by immersing the P(NIPAM-PBA) microgel monolayers in FITC-insulin solution at 4 °C for 1h. FITC-insulin solution with a concentration of 0.5 mg/mL was prepared using 50 mM pH 8.5 phosphate buffer. The weight percentage of loading was estimated to be ~19% from the increase in monolayer weight. Its release kinetics was measured in a similar way as ARS instead that the concentration of FITC-insulin were measured using fluorescence spectroscopy.

3. Results and discussion

3.1. Synthesis of P(NIPAM-PBA) microgels with big size

It is well known that PNIPAM microgels undergo phase transition at the lower critical solution temperature (LCST) of the PNIPAM

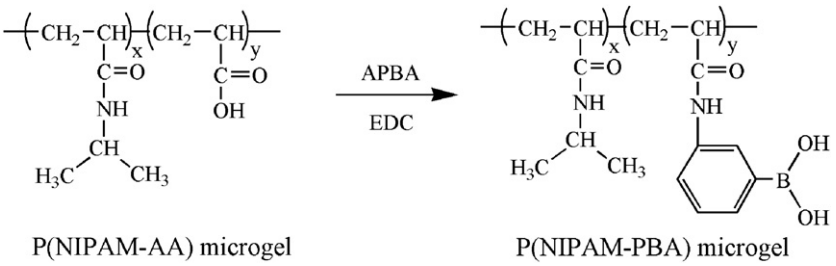

Scheme 1. Synthesis of glucose-sensitive P(NIPAM-PBA) microgels with pendant PBA groups.

polymer [23,24]. By introducing PBA groups, the resultant microgels are not only thermosensitive, but also glucose-sensitive. There are two approaches to synthesize PBA-containing PNIPAM microgels. We [7] and T. Hoare et al. [9] synthesized P(NIPAM-PBA) microgels via the modification of P(NIPAM-AA) microgels with APBA under EDC catalysis, as shown in Scheme 1. The microgels can also be synthesized by the direct copolymerization of NIPAM and 3-acrylamidophenylboronic acids as V. Ravaine et al. [8] and G. Zhang et al. [25] described. However, the microgels synthesized using the second approach present very complicated behaviors in terms of thermo- and glucose-sensitive behaviors. In contrast, P(NIPAM-PBA) microgels synthesized using the first approach show distinguished thermo- and glucose-sensitive behaviors. According to T. Hoare et al. the radial and intrachain distributions of functional groups within the three dimensional microgel network influence significantly the behavior of a microgel [14,26]. The P(NIPAM-PBA) microgels from the first approach may benefit from a relatively even distribution of the PBA functional groups which is inherited from the parent P(NIPAM-AA) microgels, while the microgels from the second approach may present complicated heterogeneous microstructures.

In this work we synthesized P(NIPAM-PBA) microgels using the same approach, however, the parent P(NIPAM-AA) microgels were synthesized in the absence of surfactant. These microgels are much bigger in size than the P(NIPAM-AA) microgels we synthesized in the previous work [7]. As shown in Fig. 1, at pH 3.5 and 25 °C the hydrodynamic radius (R_h) of the new P(NIPAM-AA) microgels is 424 nm, which is 2-fold larger than the microgel with similar composition but prepared in the presence of surfactant [7]. However, both microgels present a volume phase transition temperature (VPTT) at about 31 °C. The P(NIPAM-AA) microgels were treated with an APBA/EDC mixture in the same way as we reported previously [7]. The thermosensitive behavior of the resultant P(NIPAM-PBA) microgels was studied in 50 mM pH 8.5 phosphate buffer. As shown in Fig. 1, the phase transition of the resultant P(NIPAM-PBA) microgels occurs at about 18 °C, which is similar with the small P(NIPAM-PBA) microgels of the same composition [7]. Note the carboxylic acid groups are protonated at pH 3.5 while PBA groups are partially disassociated at pH 8.5. The shift of the microgel VPTT is attributed to the replacement of the hydrophilic monomer acrylic acid with the hydrophobic 3-acrylamidophenylboronic acid. At fully collapsed state, the P(NIPAM-PBA) microgels have the same size with the parent P(NIPAM-AA) microgels, however, at a swollen state, the P(NIPAM-AA) microgel is larger than the corresponding P(NIPAM-PBA) microgel. This result suggests that the hydrophobic comonomer in P(NIPAM-PBA) microgel also reduces its swelling degree at temperature lower than its VPTT. In contrast to the sharp phase transition of the parent P(NIPAM-AA) microgel, the phase transition of P(NIPAM-PBA) microgel is rather wide. Close examination reveals that the phase transition of P(NIPAM-PBA) microgel can be divided into two stages: a quick and sharp deswelling started at about 18 °C followed by a relatively wide deswelling started at about 22 °C. The two-stage phase transition may be explained by the heterogeneous structure of the microgel. Here the parent P(NIPAM-AA) microgel was prepared by precipitation polymerization, in which the cross-linker BIS incorporates into the microgel faster than the monomer NIPAM [27], resulting in a radial distribution of BIS in the microgel [28]. The heterogeneous structure can be described as a core/shell structure with a relatively BIS-rich "core" and a relatively BIS-poor "shell" [29]. The P(NIPAM-AA) microgel synthesized here can also be described as a core/shell structure with a BIS-rich (and so AA-poor) "core" and a BIS-poor (and so AA-rich) "shell". However, since both BIS and AA content have little effect on the LCST of PNIPAM, the VPTT difference between the "core" and the "shell" is negligible, therefore the P(NIPAM-AA) microgel presents only one phase transition. However, when AA is replaced with PBA group, which lowers the LCST significantly, the VPTT difference between the "core" and the "shell" is increased. As a result a two-stage phase transition was observed for the P(NIPAM-PBA) microgels.

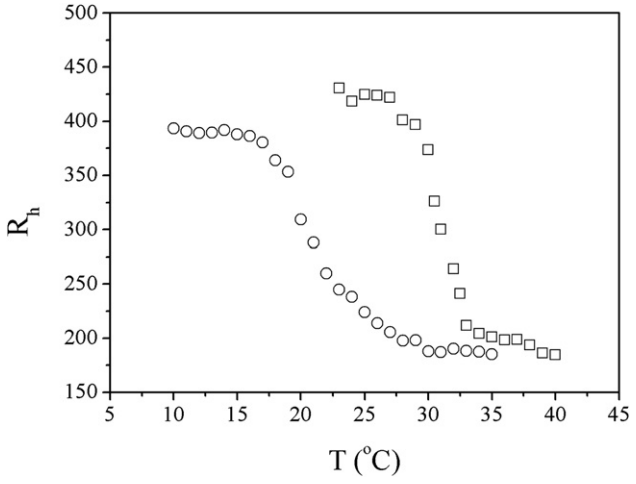

Fig. 1. Temperature dependence of the R_h values of the P(NIPAM-AA) microgels (10.0 mol% AA; pH3.5; square) and the corresponding P(NIPAM-PBA) microgels (10.0 mol% PBA; pH 8.5; circle), measured at a scattering angle $\theta = 90°$.

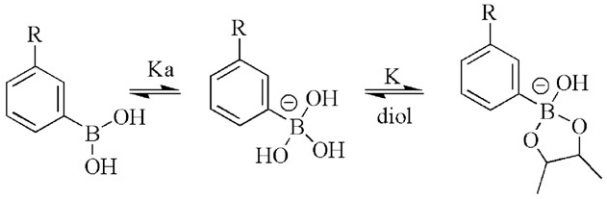

Scheme 2. Complexation equilibrium between PBA derivative and 1,2-diol.

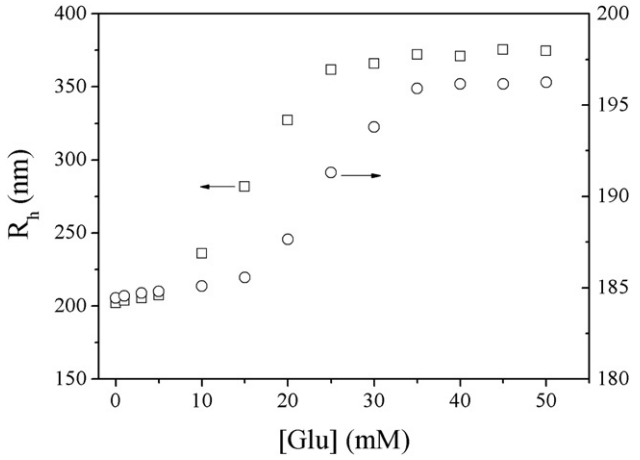

Fig. 2. Average R_h values of the P(NIPAM-PBA) microgels (10.0 mol% PBA) as a function of glucose concentration, measured in 50 mM pH 8.5 phosphate buffer at 25 °C (□) and 37 °C (○).

It is well-known that PBA group binds with a 1,2-diol, such as glucose, and forms phenylboronate ester as shown in Scheme 2 [3,30]. In the presence of glucose, the hydrophobic PBA group will be converted to negatively charged, hydrophilic phenylboronate ester. Therefore the microgel size should increase with increasing glucose concentration in the media. We have shown the glucose-induced swelling of the small size P(NIPAM-PBA) microgels at pH 8.5 and 25 °C [7]. The R_h of the new P(NIPAM-PBA) microgels as a function of glucose concentration under the same conditions was plotted in Fig. 2. At a low glucose concentration (<5 mM), no significant changes in the particle size was observed. Glucose-induced size-expanding was observed only when glucose concentration is higher than 10 mM, beyond which the microgel size increases continuously and levels off at [Glu] = 25 mM. The different behavior of the new P(NIPAM-PBA) microgels may be explained by the core-shell-like heterogeneous structure and the special binding modes of glucose with PBA groups. When glucose binds with PBA groups in alkaline aqueous solutions, they may form a glucose-mono(boronate) complex (Scheme 2), or a glucose-bis(boronate) complex, in which one glucose molecule is complexed with two PBA groups [31–33]. When glucose concentration is low, the major product in the core area should be glucose-bis(boronate) complex, because the high cross-link density is favorable for its formation [7]. In contrast, the glucose-mono(boronate) complex should be the major product in the shell area because of its low cross-link density. The formation of glucose-bis(boronate) complex increases the cross-linking density of the core area, thus reduces the particle size, however, the formation of glucose-mono(boronate) increases the charge density in the shell, which will result in an increased particle size. As a combined result of the two opposite effects of glucose binding, the particle size does not change significantly at low glucose concentration. As glucose concentration increasing, glucose-mono(boronate) complex becomes the major product for both core and shell. Therefore particle size increases with increasing glucose concentration. Effect of glucose on the particle size at 37 °C follows the same trend, however, the glucose-induced swelling is much smaller.

3.2. Synthesis of P(NIPAM-PBA) microgel monolayers

P(NIPAM-AA) microgel monolayer was fabricated on both silicon wafers and quartz slides according to Vincent et al. [22]. The negatively charged microgel particles were assembled onto the PEI-modified substrates via electrostatic interaction. The following treatment in APBA/EDC mixture converts the P(NIPAM-AA) microgel monolayer to a P(NIPAM-PBA) microgel monolayer (Scheme 1). Under EDC catalysis, amide bonds also forms between the surface carboxylic acid groups and the amino groups of the substrate. As a result the P(NIPAM-PBA) microgel spheres are covalently attached on the substrate. These films are highly stable. We did not observe any desorption of microgel spheres in the following drug loading and release experiments.

SEM image of the P(NIPAM-AA) microgel monolayer reveals dense packing of the microgel particles within the monolayer (Fig. 3, left), which is in agreement with Vincent et al. [22]. The microgel particles are highly monodisperse with an average diameter of 540 nm. A size shrinkage was observed when the P(NIPAM-AA) microgels were converted to P(NIPAM-PBA) (Fig. 3, right), which is in agreement with the observation in solution (Fig. 1). Fig. 4 shows the FTIR spectra of the microgel monolayer before and after PBA modification. The disappearance of the carboxylic acid peak at 1709 cm^{-1} suggests that almost all of the carboxylic acid groups were reacted with APBA.

3.3. Loading and release of ARS

The successful fabrication of P(NIPAM-PBA) microgel monolayers provides a good basis for the study of drug loading and release behavior of the microgel particles. When immersed in a solution, the environment of the attached particles is similar to that of the dispersed ones. The effect of the solid substrate on the thermo- and glucose-sensitive behavior is expected to be

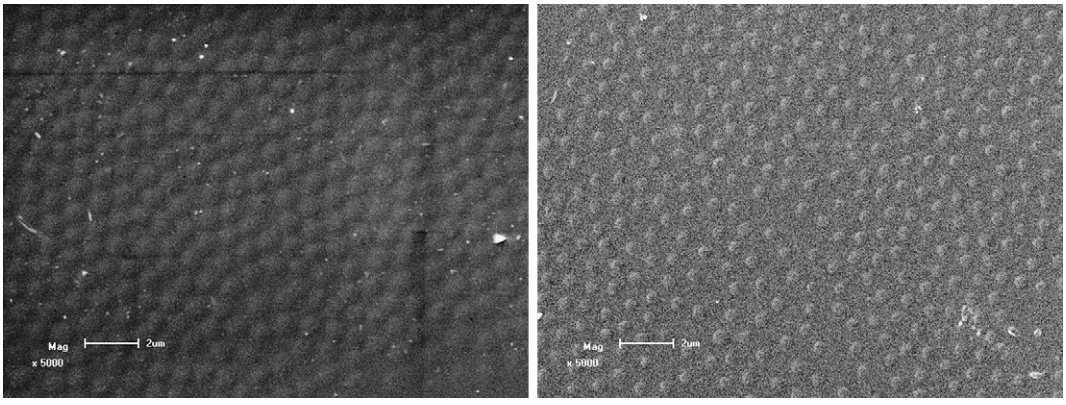

Fig. 3. SEM images of P(NIPAM-AA) (left) and P(NIPAM-PBA) (right) microgel monolayers. Scale bar = 2 μm.

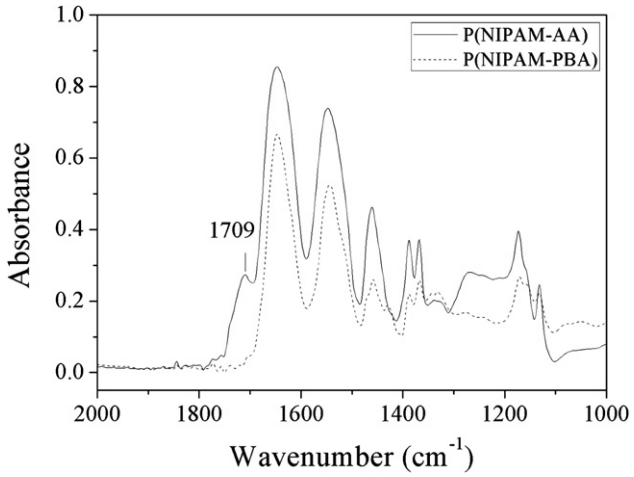

Fig. 4. FTIR spectra of the P(NIPAM-AA) microgel monolayer (solid line) and the corresponding P(NIPAM-PBA) microgel monolayer (dash line).

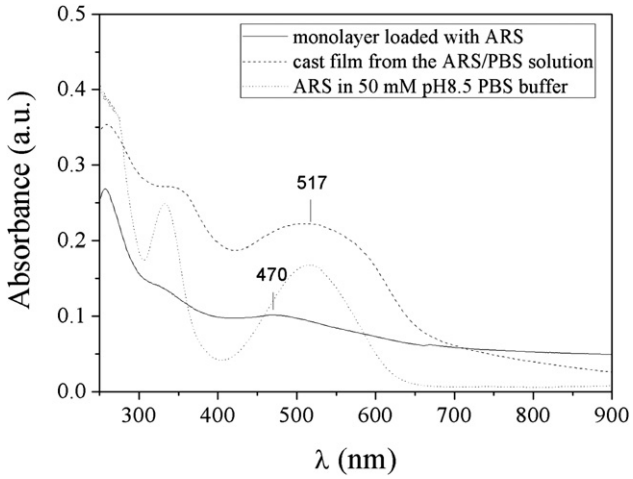

Fig. 5. Absorption spectra of a monolayer loaded with ARS (solid line), ARS in 50 mM pH 8.5 phosphate buffer (dot line) and a cast film from the ARS/phosphate buffer solution (dash line).

negligible. Previously, Vincent et al. revealed that the thermosensitive behavior of monolayer from PNIPAM microgel without bulk ionisable comonomer groups is similar to that of the free particles [22]. Here ARS and FITC-insulin were chosen as model drugs. ARS was chosen because it has a 1,2-diol structure which may represent drugs that can bind with the monolayer through reversible phenylboronate ester bonding (Scheme 3), such as glycosylated insulin [34]. Glucose-controlled release of this type of drugs may be achieved because glucose may compete with the drugs for binding sites in the microgels.

ARS was loaded by immersing the microgel monolayers in aqueous solution of ARS. The absorption spectra of a microgel monolayer loaded with ARS was shown in Fig. 5. For comparison, the spectra of ARS in phosphate buffer and a cast film from the ARS/phosphate buffer solution are also presented. Compared with ARS in solution and the cast film, when loaded in the microgel monolayer, the absorption band of ARS shifts from 517 nm to 470 nm, indicating that most of the dye adsorbed in the monolayer binds with the PBA groups (Scheme 3). The hypsochromic shift of the ARS band upon complexation with PBA in aqueous solutions has been reported previously in the literature [35].

Fig. 6 shows the loading kinetics of ARS at 13 °C. The loading amount of ARS is represented by the absorption increase of the film at 263 nm. As can be seen, the loading of ARS is quick and reaches equilibrium within 5 min regardless of the ARS concentration in the loading solutions. Fig. 6 also shows that as the ARS concentration increases the loading amount of ARS increases accordingly. This can be explained by the equilibrium shift of the reaction between PBA groups and ARS as the ARS concentration increases, resulting in more ARS/PBA complex forms in the monolayer (Scheme 3).

The effect of temperature on the loading capacity of the P(NIPAM-PBA) microgel monolayer was studied. As shown in Fig. 7, the loading amount of ARS increases as temperature decreases from 20 °C to 5 °C. This result is parallel to the increasing swelling degree of the microgels. The swelling of the microgel particles permits ARS molecules to diffuse into the particle interior and react with PBA groups. Indeed, at the temperature range of 20–30 °C, as the microgel particles are fully collapsed, the loading amount of ARS is negligible. However, when further increasing temperature, the loading amount of ARS increases slightly. Under these conditions ARS may be adsorbed to the particle surface through hydrophobic interaction which is enhanced at high temperature.

The above studies indicate that the microgel monolayer has a larger loading capacity at low temperature and the ARS loading reaches equilibrium in 5 min. Therefore for the following studies, ARS was loaded by immersing the monolayer films in 10 mM ARS solution at 4 °C for 1 h. The ARS-loaded films were then immersed in various release media to study the drug release behaviors.

Fig. 8 compares the release profiles of ARS at various temperatures. In all cases, a quick initial release was observed. The result is reasonable considering the small size of the microgel particles and hence a relatively large surface area. When temperature increases from 15 °C to 37 °C, both the initial release rate and the total released amount of ARS increases with increasing temperature, however, at 4 °C the total released amount is the highest in all the

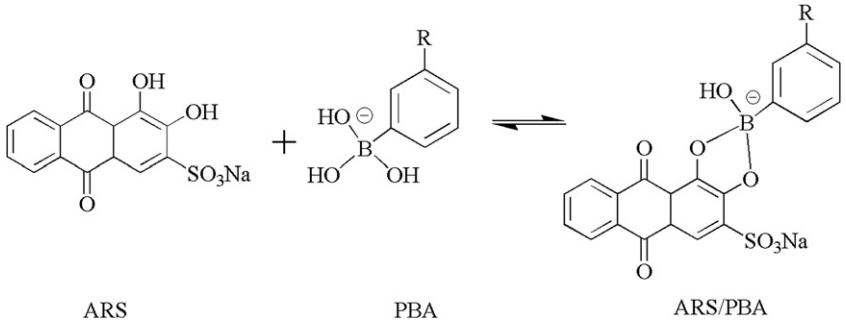

Scheme 3. Structure of ARS and its binding with PBA group.

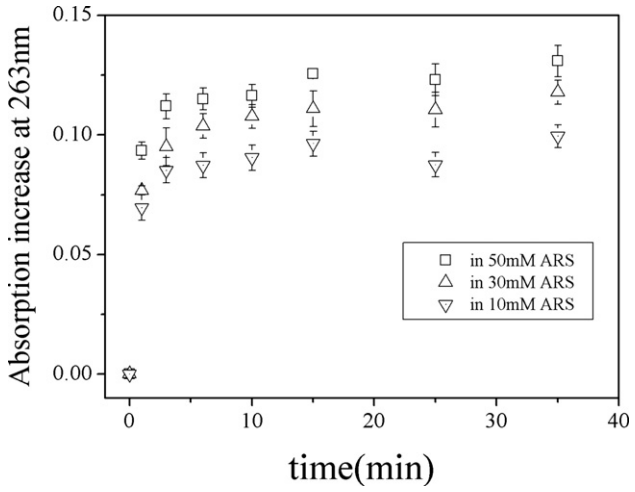

Fig. 6. Loading kinetics of ARS in different ARS solution in phosphate buffer (50 mM pH = 8.5) at 13 °C. The loading amount of ARS was represented by the absorption increase of the microgel monolayer at 263 nm.

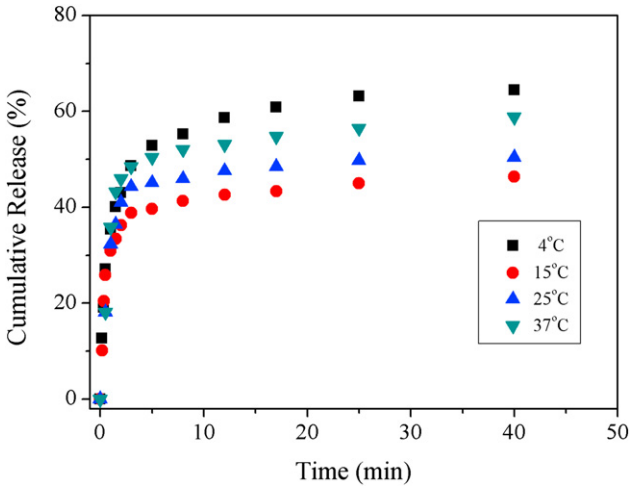

Fig. 8. Release profiles of ARS at various temperature. The release medium was 20 mL of phosphate buffer (50 mM pH 8.5).

cases, although the initial release rate is somewhat slower than that at 37 °C.

The most common mechanism of drug release from hydrogels is passive diffusion, and the drug diffusion out of a hydrogel matrix is primarily dependent on the mesh sizes within the matrix of the gel [36]. For thermosensitive PNIPAM hydrogels or microgels, as they undergo rapid phase transition at temperature higher than their VPTT, drug will be released through a "squeeze-out" mechanism [37]. Note that in this study the drugs were loaded at 4 °C and then the monolayers were transferred into release media of various temperatures. When released at 4 °C, since temperature does not change, so does the swelling degree of the microgel particles. The release of ARS should be a simple passive diffusion process. At this temperature the microgel particles are fully swollen. The mesh size of the particle must be large enough for the quick diffusion of ARS, which is a small molecule. When released at 15 °C, the microgel particles will just shrink slightly. Therefore the squeezing effect should be negligible. ARS should be released mainly by passive diffusion. However, since the temperature is close to VPTT of the microgels, it is likely that the periphery of the particles, which has a VPTT lower than the interior part, collapses immediately when contact with the warm medium. The collapsed periphery forms a dense "skin" layer, which reduces the release rate of ARS significantly. The lower VPTT of the microgel periphery originates from the heterogeneous structure, because of which the phase transition of PNIPAM microgels usually starts from the periphery and follows an "outside-in" mechanism [38,39]. When release at a temperature higher than the VPTT, a dense skin layer also forms, however, as the microgel particles experience abrupt and drastic shrinkage, the loaded drug can be "squeezed" out [37]. Therefore, drug releases at a higher speed. Because the extent and the rate of phase transition increase with temperature, the drug release rate and the released amount increase with increasing temperature too. The different drug release mechanisms at different temperatures were depicted schematically in Scheme 4.

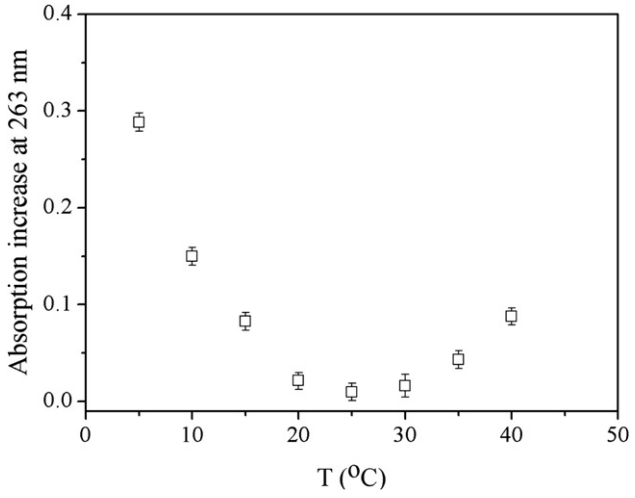

Fig. 7. Loading amount of ARS as a function of temperature in 10 mM ARS solution in 50 mM pH 8.5 phosphate buffer. The loading amount of ARS was represented by the absorption increase of the microgel monolayer at 263 nm.

Fig. 9 shows the effect of glucose on the release kinetics at 4 °C and 37 °C, which is below and above the VPTT of the P(NIPAM-PBA) microgels, respectively. In both cases, both the release rate and the total released amount of ARS increases with increasing glucose concentration in the release media. Same trend was found when release at 15 °C and 25 °C (data not shown). As mentioned above, The ARS release at 4 °C is governed by diffusion. The enhanced release of ARS can be attributed to the competition of glucose with ARS for binding with PBA groups. In the presence of glucose, the free PBA groups will be partially consumed by binding with glucose. Therefore the equilibrium among the free PBA, ARS, and PBA/ARS complex, as shown in Scheme 3, will shift to the left. As a result, more ARS will be released to the media. The increased ARS concentration gradient in the presence of glucose also results in a higher release rate.

At temperatures higher than VPTT where ARS is squeezed out, the effect of glucose may be quite complicated. On one hand, as glucose binds with the PBA groups and converts PBA groups from a hydrophobic neutral form to hydrophilic, negatively charged form, the VPTT of the microgels will increase. The extent of the phase transition will be lower, and the temperature-induced squeeze effect will decrease. On the other hand, the competition of glucose with ARS for PBA binding site will enhance the release of ARS, as we analyzed above. From Fig. 9B, the second effect of glucose dominates the first one, therefore the release of ARS increases with increasing glucose concentration.

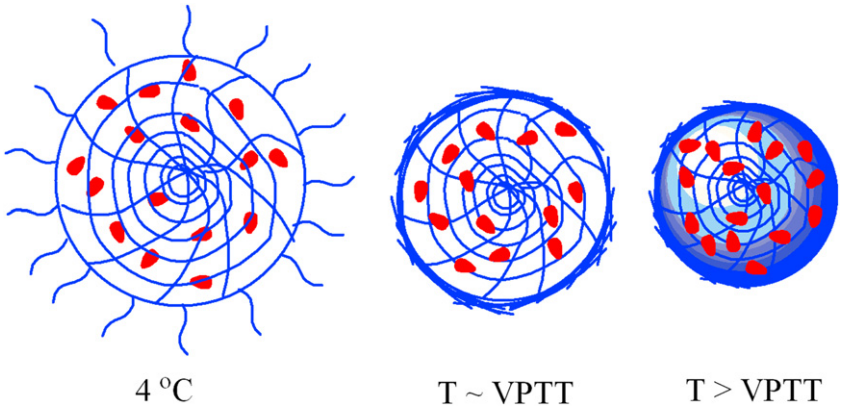

Scheme 4. Drug release mechanisms at different temperatures. At 4 °C, the drug release follows a passive diffusion mechanism. At temperature close to VPTT of the microgel, the diffusion of the drug is retarded by a thin dense "skin layer". At temperature higher than VPTT, the drugs are squeezed out due to the quick shrinkage of the microgel particle.

From Fig. 9, the release amount of insulin at 4 °C is larger than that at 37 °C in all media. This result is in agreement with that shown in Fig. 8. Possible reason may be the formation of "skin layer" retard the release of ARS at high temperature.

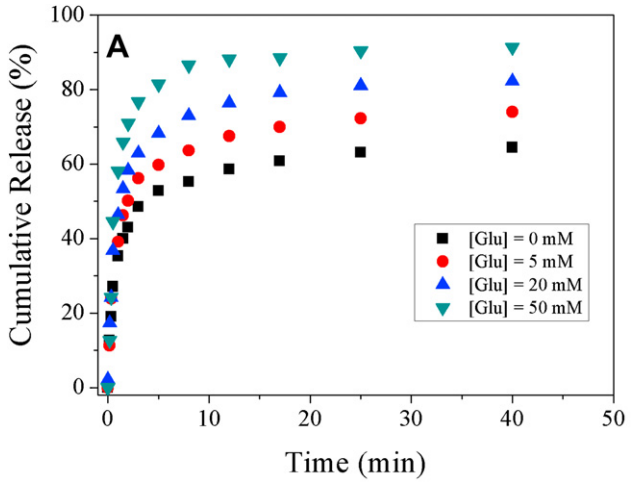

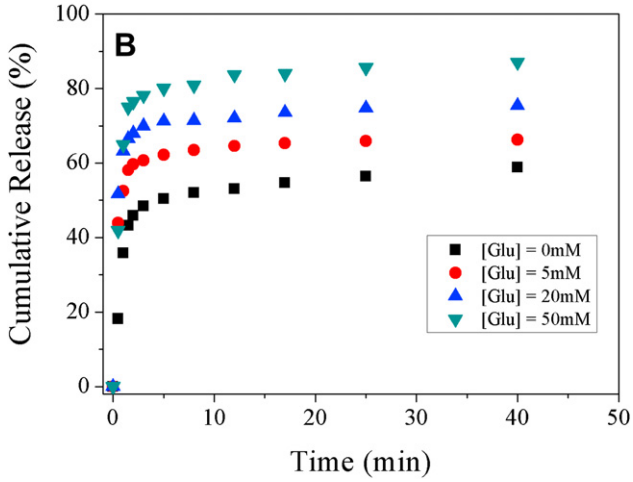

Fig. 9. Release profiles of ARS in phosphate buffer (50 mM, pH 8.5) containing various concentrations of glucose. Temperature is 4 °C for A and 37 °C for B, respectively.

3.4. Loading and release of FITC-insulin

FITC-insulin was loaded in the same manner. Its release profiles at various temperatures were shown in Fig. 10. The effect of temperature on the release of insulin is similar to that of ARS, i.e., the release amount of insulin decreases when temperature rises from 4 °C to 15 °C, but increases when further increasing temperature. This phenomenon can be explained in a similar way. The release of insulin at 4 °C can be simply regarded as a passive diffusion. At 15 °C, insulin release is retarded by the skin layer. However, at even higher temperatures, the release of insulin speeds up due to the squeeze-out mechanism.

Although the release of insulin and ARS follows the same general trend, they also present some different behaviors. The release amount of ARS decreases in the order of 4 °C > 37 °C > 25 °C > 15 °C (Fig. 8), while the release amount of insulin decreases in the order of 37 °C > 25 °C > 4 °C > 15 °C (Fig. 10). The different behavior may be explained by their different molecular weight. At 4 °C when both drugs are released by passive diffusion, it is easier for the release of low molecular weight ARS. Therefore the release amount of ARS is higher than that of insulin. However, when released by the squeeze-out mechanism at high temperature, insulin with a higher molecular weight can be squeezed out more effectively (Fig. 10).

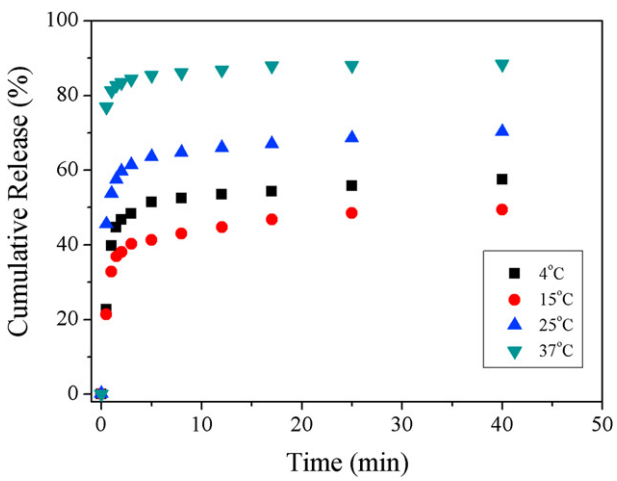

Fig. 10. Release profiles of FITC-insulin at various temperature. The release medium was phosphate buffer (50 mM pH 8.5).

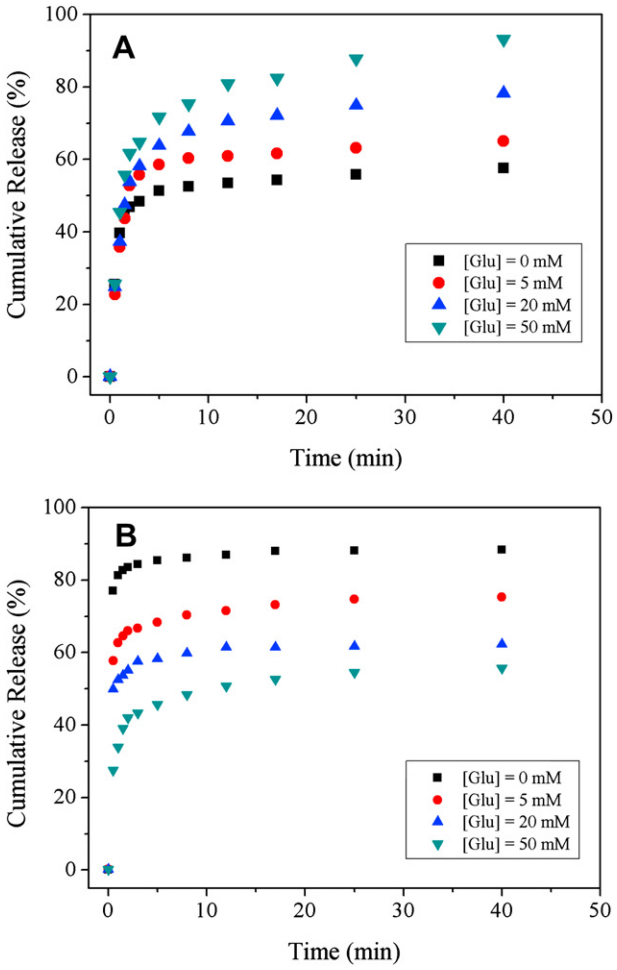

Fig. 11. Release profiles of FITC-insulin in phosphate buffer (50 mM, pH 8.5) containing glucose. Temperature is 4 °C for A and 37 °C for B, respectively.

The effect of glucose on the release of insulin at 4 °C was shown in Fig. 11A. The release amount of insulin increases with increasing glucose concentration in the release media, indicating glucose enhances the passive diffusion of insulin by increasing the swelling extent of the microgel particles. However, at 37 °C an opposite trend was observed: the released amount of insulin decreases with increasing glucose concentration (Fig. 11B). At this temperature insulin was released through a squeeze-out mechanism. The glucose-induced swelling of microgel particles moderates this effect, therefore reduces the released amount of insulin. This result is unexpected, because for practical application, the released amount of insulin should increase with increasing glucose concentration.

The results shown in Fig. 11B also reveal that microgel and bulky gel of the same composition may behave differently. Previously Kataoka et al. observed increased insulin release from P(NIPAM-PBA) bulky gel upon exposing to glucose at 28 °C [3]. In this case the release of insulin was regulated through the formation and disruption of the surface barrier layer of the gel.

4. Conclusions

In conclusion, we synthesized P(NIPAM-PBA) microgels with size bigger than the one we synthesized previously. The new microgels also exhibit glucose-sensitive behaviors. Novel P(NIPAM-PBA) microgel monolayers were prepared, which provide a good basis for the study of drug loading and release behavior of colloidal microgel particles. At low temperature, the drug release follows a passive diffusion mechanism, but with increasing temperature, the drug is released mainly by a squeeze-out mechanism. For drugs can bind with PBA groups through reversible phenylboronate ester bonds, glucose enhances their release at all temperatures, however, for drugs have no specific interaction with the microgel, glucose enhances their release at low temperature, but retards at high temperature.

These results will guide the design of new self-regulated insulin release systems based on P(NIPAM-PBA) microgels. The drug release mechanisms revealed here suggest two ways to achieve this goal. The first one is to modify insulin with diol structures, so it can bind with PBA groups through reversible phenylboronate ester bonds. Glucose will enhance its release by competing for PBA binding site. The second way is to create a core-shell structure, in which the drug is loaded in the core, while the glucose-sensitive shell will control the release of the drug. Both strategies are under active investigation in our lab.

Acknowledgments

We thank financial support for this work from the National Natural Science Foundation of China (Grant Nos.: 20774049 and 20974050), Ministry of Science and Technology of China (Grant No.: 2007DFA50760) and Tianjin Committee of Science and Technology (Grant No. 07ZCGHHZ01200).

References

[1] Kost J, Langer R. Adv Drug Deliver Rev 2001;46:125–48.
[2] Miyata T, Uragami T, Nakamae K. Adv Drug Deliver Rev 2002;54:79–98.
[3] Kataoka K, Miyazaki H, Bunya M, Okano T, Sakurai Y. J Am Chem Soc 1998;120:12694–5.
[4] Ding Z, Guan Y, Zhang Y, Zhu XX. Polymer 2009;50:4205–11.
[5] Matsumoto A, Ikeda S, Harada A, Kataoka K. Biomacromolecules 2003;4:1410–6.
[6] Matsumoto A, Yoshida R, Kataoka K. Biomacromolecules 2004;5:1038–45.
[7] Zhang Y, Guan Y, Zhou S. Biomacromolecules 2006;7:3196–201.
[8] Lapeyre V, Gosse I, Chevreux S, Ravaine V. Biomacromolecules 2006;7:3356–63.
[9] Hoare T, Pelton R. Macromolecules 2007;40:670–8.
[10] Liu Y, Zhang Y, Guan Y. Chem Commun 2009;14:1867–9.
[11] Hoare T, Pelton R. Biomacromolecules 2008;9:733–40.
[12] Lapeyre V, Ancla C, Catargi B, Ravaine V. J Colloid Interf Sci 2008;327:316–23.
[13] Zhang Y, Guan Y, Zhou S. Biomacromolecules 2007;8:3842–7.
[14] Hoare T, Pelton R. Langmuir 2008;24:1005–12.
[15] Nerapusri V, Keddie JL, Vincent B, Bushnak LA. Langmuir 2007;23:9572–7.
[16] Soppimath KS, Tan D, Yang YY. Adv Mater 2005;17:318–23.
[17] Kiser PF, Wilson G, Needham D. Nature 1998;394:459–62.
[18] Nolan CM, Serpe MJ, Lyon LA. Biomacromolecules 2004;5:1940–6.
[19] Serpe MJ, Yarmey KA, Nolan CM, Lyon LA. Biomacromolecules 2005;6:408–13.
[20] Bromer WW, Sheehan SK, Berns AW, Arquilla ER. Biochemistry 1967;6:2378–88.
[21] Pelton RH, Chibante P. Colloids Surf 1986;20:247–56.
[22] Nerapusri V, Keddie JL, Vincent B, Bushnak IA. Langmuir 2006;22:5036–41.
[23] Zhang J, Chu LY, Cheng CJ, Mi DF, Zhou MY, Ju X. J Polym 2008;49:2595–603.
[24] Piperno S, Gheber LA, Canton P, Pich A, Dvorakova G, Biffis A. Polymer 2009;50:6193–7.
[25] Ge H, Ding Y, Ma C, Zhang G. J Phys Chem B 2006;110:20635–9.
[26] Hoare T, McLean D. J Phys Chem B 2006;110:20327–36.
[27] Wu X, Pelton RH, Hamielec AE, Woods DR, McPhee W. Colloid Polym Sci 1994;272:467–77.
[28] Varga I, Gilanyi T, Meszaros R, Filipcsei G, Zrinyi M. J Phys Chem B 2001;105:9071–6.
[29] Saunders BR. Langmuir 2004;20:3925–32.
[30] Ding Z, Guan Y, Zhang Y, Zhu XX. Soft Matter 2009;5:2302–9.
[31] Shiomi Y, Saisho M, Tsukagoshi K, Shinkai S. J Chem Soc Perkin Trans 1 1993;17:2111–7.
[32] Eggert H, Frederiksen J, Morin C, Norrild JC. J Org Chem 1999;64:3846–52.
[33] Alexeev VL, Sharma AC, Goponenko AV, Das S, Lednev IK, Wilcox CS, et al. Anal Chem 2003;75:2316–23.
[34] Liu F, Song SC, Mix D, Baudys M, Kim SW. Bioconjugate Chem 1997;8:664–72.
[35] Springsteen G, Wang BH. Tetrahedron 2002;58:5291–300.
[36] Hamidi M, Azadi A, Rafiei P. Adv Drug Deliver Rev 2008;60:1638–49.
[37] Wu JY, Liu SQ, Heng P, Yang YY. J Control Release 2005;102:361–72.
[38] Wu C, Zhou S. Macromolecules 1997;30:574–6.
[39] Gan DJ, Lyon LA. J Am Chem Soc 2001;123:8203–9.